◆◆ **Scientific**
◆◆ **Research**

Male Breast Cancer-Dosimetry Evaluation in Teletherapy

Nilmara A. Guimarães*, Verginia R. Crispim

Universidade Federal do Rio de Janeiro, UFRJ/CT/COPPE/Programa de Engenharia Nuclear, Rio de Janeiro, Brazil
Email: *nilaguimaraes@hotmail.com

Abstract

The rate of male breast cancer has increased in recent years, due to the deficiency of preventive examinations (male mammography). Besides, since male breasts are generally smaller than female breasts, it is essential to monitor the doses received by male breasts, as well as those received by close, healthy and critical organs in order to assess the plan used in this kind of treatment. To do this, the distribution of doses in male breasts was simulated and assessed, based on the procedures adopted in the treatment of female breasts, when submitted to a radiation beam from a linear accelerator. The Alderson Rando phantom was used and the relevant absorbed doses were measured by TLD-100 thermoluminescent dosimeters distributed throughout the volume of interest. The results of the treatment planning were compared with the results obtained by TLDs. A difference of up to 8.5%, in comparison with the planned dose, as well as a 6% relative standard deviation was found.

1. Introduction

The second most lethal cancer in the world is breast cancer, which can also affect men [1] [2] and which, as more unusual, is not much studied. It represents about 1% of all breast cancers, accounting for less than 0.1% of deaths in men [3] [4].

Cancer may be treated in various ways, through: surgery, chemotherapy, radiotherapy or a combination thereof. In the absence of proper protocols, the recommended treatment for male breast cancer follows the treat-

_____

*Corresponding author.

ment established for female breast cancer, based on surgical treatment, combined or not with radiotherapy, chemotherapy, and especially hormonal therapy [5]. Since the structure and volume of male breasts may be different from those of female breasts, radiotherapy must also be different in terms of distributed doses.

1.1. Radiotherapy through Teletherapy

In teletherapy, the radiation issued by the applicable device is targeted at the body region to be treated, while patient is lying down, and sessions are performed daily. Cobalt therapy machines (^{60}Co) and linear accelerators are the equipment used.

1.2. Dose Distribution

The distribution of doses refers to the dose values at points surrounding and inside the irradiated volume. In radiotherapy, a detailed analysis of the dose distribution allows drawing conclusions with respect to the preservation of healthy tissues near the target volume. Thus, it is important to make sure that the doses prescribed by physicians focus on the target volumes, so that healthy tissues do not receive doses beyond the tolerance limits recommended in literature.

1.3. Ionizing Radiation Dosimeters

The result of measurement is a dosimetric amount expressed by a number associated with its unit. There are several types of radiation dosimeters, but not all meet the necessary requirements for the intended application. Thus, it is necessary to choose the most appropriate one, taking into account the requirements of the measurement situation. Among the types of dosimeters on the market, we shall highlight: ionization chamber, radiographic film, radiochromic film, thermoluminescent dosimeter (TLD) and semiconductors (diode) [6].
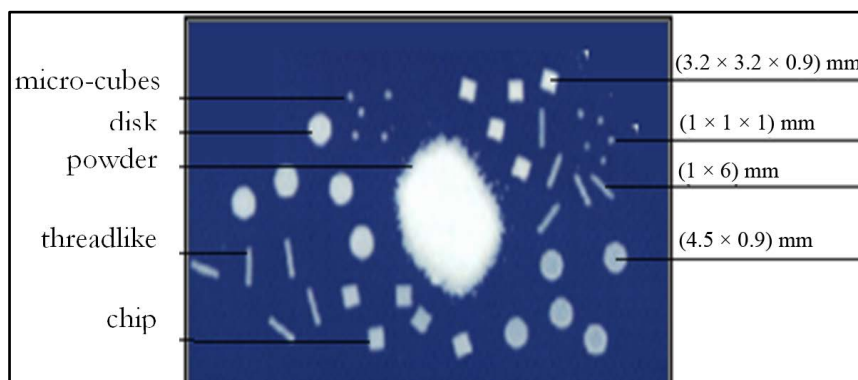
1.4. Thermoluminescent Dosimeter

The thermoluminescent dosimeter is a device that measures doses resulting from the thermoluminescence phenomena, which occurs when there is light emission after the excitation of a material medium by thermal energy. Light emission may result by fluorescence, when light emission occurs spontaneously, and by phosphorescence, when it is necessary to apply energy for it to be seen. TL dosimeters can be found in various shapes and compositions, as shown in **Figure 1**.

Among the main TL dosimeters, we shall highlight: LiF: Mg, Ti; CaF_2: Dy; CaSO4: Dy; CaF_2: Mn; LiF: Mg, P, Cu; and $Li_2B_4O_7$: Mn. The chip dosimeter, composed of lithium fluoride, is generally the most widely used in dosimetry, as it is easily manipulated, and presents good repeatability and reproducibility conditions.

2. Materials and Methods

To characterize and calibrate TLD thermoluminescent dosimeters, irradiations were performed at a known dose rate in the teletherapy equipment ONCOR Expression, manufactured by SIEMENS, installed at COI (for the acronym in Portuguese for Integrated Oncology Centers). The accelerator used in the characterization was the

Figure 1. Types of thermoluminescent dosimeters (Taken from [7]).

same used for irradiation, namely, a 6.0 mV photon beam and, therefore, it was not necessary to determine the energy dependence factor.

The thermoluminescent dosimeters used were TLD-100 (LiF: Mg, Ti), in the shape of chip, measuring 3.2 mm × 3.2 mm × 0.9 mm, manufactured by Thermo Fischer Scientific Inc., commercially known as Harshaw TLD (**Figure 2**).

For proper use of TLDs, it was necessary to determine their individual characteristics. Among the group of TLDs, those which met the characteristics identified by the manufacturer were identified, and the relevant provided quality controls were obtained through sampling.

The steps followed for the selection of chips suitable for dose measurements require knowledge of each chip specifically and include:

Univocal identification of TLD;

Thermal pre-treatment;

Response "Zero", corresponding to the condition "not irradiated", also known as "BG" level (background);

Evaluation of sensitivity;

Evaluation of linearity according to calibration;

Assessment of other correction factors: time, transportation and energy dependence, which were not necessary in this case.

Since TLDs were not brand new, after being identified, they were heat treated at 400°C for one hour, and at 100°C, for two hours, in order to remove any residual dose previously applied.

2.1. Stacking and Reading of TLDs

After the initial heat treatment, these TLDs were inserted in *coupelles* to be read, organized in a predefined reading order and stacked with the assistance of a lift. A twelve hour interval to perform new radiations was taken into account. Once stacked, so that measures found in each TLD could be tracked, they were placed in a Fimel PCL3 reader. As such, the BG values of the 200 TLDs examined were determined. The mean reading of the "zero dose" (TL_0) was obtained through the mean of the readings of the 200 TLDs by Equation (1). The measurement uncertainty associated with this parameter was the standard deviation of the 200 readings.

$$\text{TL}_0 = \sum_{I=0}^{200} \text{TL}_0 \tag{1}$$

The reader's charger was able to stack up to 93 *coupelles*, or 93 chips (TLDs). The reader had a system which included a rotating disk and tweezers that removed every *coupelle* from the charger and took it to oven no. 1, to oven no. 2, to the photomultiplier valve and, finally, placed it in a disposal charger. In oven no. 1, the *coupelle* was submitted to a temperature of 170°C for about 25 seconds and, in oven no. 2, to a temperature of 300°C for about 25 seconds. At this point, the photomultiplier valve recorded the light photons resulting from the release of electrons that were caught up in the TLDs' traps.

Figure 2. TLD-100 within the *coupelle*.

2.2. Evaluation of Sensitivity

To determine the relative sensitivity of TLDs, the homogeneity of the field was ensured, by irradiating them at the same time, between solid water plates, as illustrated in **Figure 3**. A distance of 100 cm between the source and the plate surface was established, together with a 20 cm × 20 cm irradiation field and a reference dose of 1 Gy.

The relative sensitivity of each TLD is defined by Equation (2), where: N is the number of evaluated TLDs; k is the number of irradiations performed; and TL_i, k is the reading of each TLD, after deducting the corresponding BG.

$$S_{i,k} = \frac{TL_{i,k}}{\frac{1}{N}\sum_{i=1}^{N} TL_{i,k}} \tag{2}$$

2.3. Evaluation of Linearity

To evaluate the linearity, the 200 TLDs were divided into 10 batches initially identified by letters, and each batch received the following doses: (10, 50, 100, 150, 200, 250, 300, 350, 400 and 500) cGy. Each batch was irradiated three times and the dose-response relation (RDS) was calculated for each batch.

Using the Excel program, a graph of the Linearity Factor, F_{lin}, versus the dose received for each batch, was generated with the correction of the readings of TLDs, in relation to response linearity. After completion of the characterization stage, TLDs were distributed throughout the Alderson Rando phantom, where the male breast and critical organs could be found in slices 13 to 20.

2.4. Anthropomorphic Simulators or Phantoms

Among the anthropomorphic phantoms used to reproduce the scattering and absorption characteristics of the body or body parts, when subjected to a radiation field, the best known is the Alderson Rando phantom (**Figure 4**) which consists of a skeleton covered with materials equivalent to tissues, lungs and soft tissues, and which follows the ICRU-44 standards [8].

This phantom is 175 cm tall and weighs 73.5 kg, being transected-horizontally into 2.5 cm thick slices. Each slice has holes which are plugged with tissue equivalent pins which can be equivalent to: bones, soft-tissues or lungs. Such pins may be replaced by powder or chip TLD pins. TLDs were placed throughout the left side of the phantom between slices 13 and 20, as per **Figure 5**, where 5 mm-diameter holes with TLDs can be found in 3 cm × 3 cm matrix.

Figure 3. Experimental arrangement for the characterization of TLDs using a solid plate.

Figure 4. Alderson Rando phantom.

Figure 5. Slice with TLDs and holes [9].

2.5. Male Breast Cancer Planning System

The planning system used to simulate the treatment of male breast cancer, following protocols for treatment of female breast cancer, was Prowess, Version 5.11, which is available at COI. Prowess has an algorithm that can manage information about doses, monitor units, image acquisition and fusion, as well as transport planning directly to the linear accelerator in which treatment shall occur.

Planning was done with the images of the Alderson Rando phantom taken by a Siemens Emotion Duo CT scanner installed at COI. The treatment consisted in the irradiation of two opposing parallel fields with the prescription of 200 cGy at 100% of the isodose line. During the first stage of irradiation, the head, also known as gantry was at 303˚, with a SSD (source-surface distance) of 88.1 cm, a field of 10 cm × 12 cm and a 240.7 MU monitor unit with 30˚ filter. In the second stage, the gantry rotated automatically to 123˚, with a SSD of 88.5 cm, a field of 10 cm × 11 cm and a 241.8 MU monitor unit, using the same filter.

For purposes of comparing the planned results with the ones obtained by TLDs, it was necessary to incorporate, in the planning system, some points of interest, *i.e.*, specific TLD location, as shown in **Figure 6**. Thus, it was possible to generate a report where the doses planned were determined, at the points of interest.

3. Results and Discussion

3.1. Sensitivity of TLDs

After determining the relative sensitivity of each TLD, we found 64 TLDs which repeatability was of up to ±0.5%
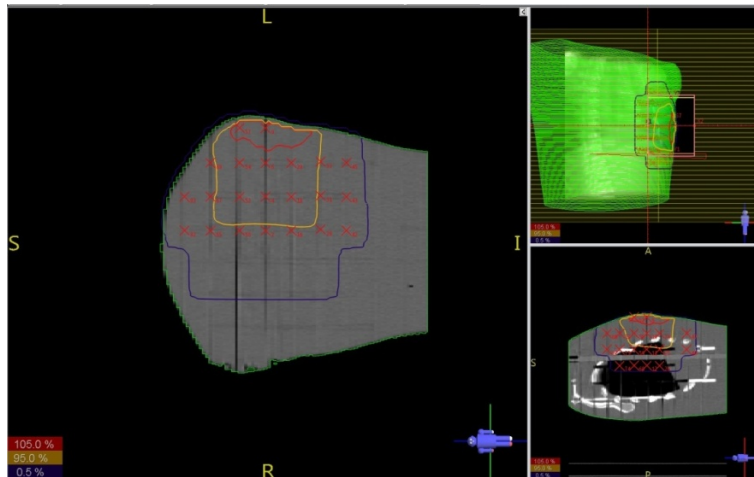
Figure 6. Prowess' Graphical Screen with the points of interest, near the male breast, located in the slices of the Alderson Rando phantom.

of standard deviation of the mean, 155 TLDs with up to ±1% of standard deviation of the mean, 197 TLDs with up to ±2% of standard deviation of the mean and three dosimeters which average standard deviation was above 3%, within the specifications of the manufacturer.

The 155 dosimeters that showed standard deviations of the mean of up to ±1% were selected for measurements.

3.2. Linearity of TLDs

To determine the response of TLDs, as a function of linearity with respect to dose, a dose range between 50 cGy and 500 cGy was taken into account. The ratio between delivered dose and TLD response was calculated for each dose chosen within the range of creation of the calibration curve. This ratio was normalized in relation to the 1 Gy reference dose, then obtaining the F_{lin} factor, as to know, the correction factor for the non-linearity of reading presented by TLD irradiated with the unknown dose.

Figure 7 shows the calibration curve obtained with the Excel program for F_{lin}.

The R-squared value found was of 0.988, which expresses how much error can be assumed by using the adjustment equation. R2 values close to 1.00 show a good quality of point adjustment to the curve and values below 0.8 indicate poor quality. It is important to note that this adjustment often introduces a doubt in F_{lin}, which can be minimized with the determination of the uncertainty due to adjustment through Equation (3). Such uncertainty must be expanded and, then, combined with the measurement uncertainty. The calculation of adjustment uncertainty will be determined by Equation (3).

$$U_{\text{ajuste}} = K \cdot \sqrt{\frac{1}{n-2} \sum \left(y_i - y_{f(x_i)} \right)^2}$$ (3)

where:

U_{ajuste} is the uncertainty of the adjustment by the equation;

K is the coverage factor, taken from the t-student table for $n-2$ degrees of freedom;

n is the number of points used to generate the equation;

y_i is the value of the error in the ith-calibrated point, used to generate the equation of linearity;

$y_{f(x_i)}$ is the value of the error in the ith-calibrated point, calculated by the linear equation.

The value found for U_{ajuste}, in Equation (3), considering a 68% reliability, referring to ±1 standard deviation, in a normal probability distribution, was 0.00015%.

This calibration curve has a considerable error for doses below 50 cGy, however, it was the best calibration curve generated in relation to the adjustment between actual and calculated points. This low adjustment uncertainty implies that such evaluated point, in relation to others, does not impact the final result of the use of the calibration curve. Nevertheless, it is necessary to observe the results found in doses of less than 50 cGy.
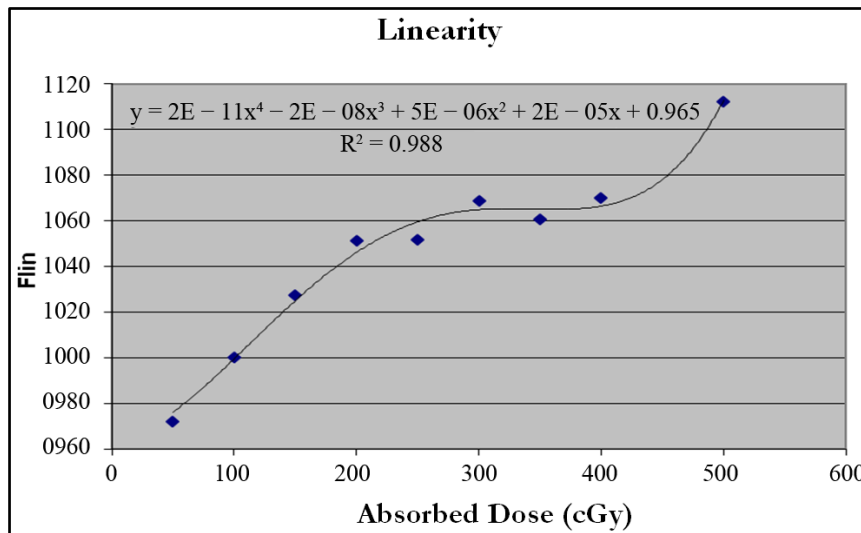
Figure 7. Curve for adjustment between TLDs' Flin and doses.

3.3. Measurement Uncertainties

The uncertainty of the dose obtained by TLDs came from the analysis of input variables and resulted from the propagation of uncertainties, Equation (4):

$$u_D^2 = \left(\frac{\partial D}{\partial L}\right)^2 u_L^2 + \left(\frac{\partial D}{\partial S}\right)^2 u_S^2 + \left(\frac{\partial D}{\partial F_{\text{lin}}}\right)^2 u_{F_{\text{lin}}}^2 \tag{4}$$

The relative uncertainty for dose D experimentally obtained with TLDs was of $\pm 0.0114\%$ or $\pm 1.14\%$.

3.4. Dosimetry with TLDs

TLDs were scattered in the form of matrix on the right side of Rando Alderson on points presenting doses different from zero, within blue, yellow and red isodoses, from slice 15 to 18, as other slices showed no significant doses. TLDs were placed on pins that had a space for chip insertion.
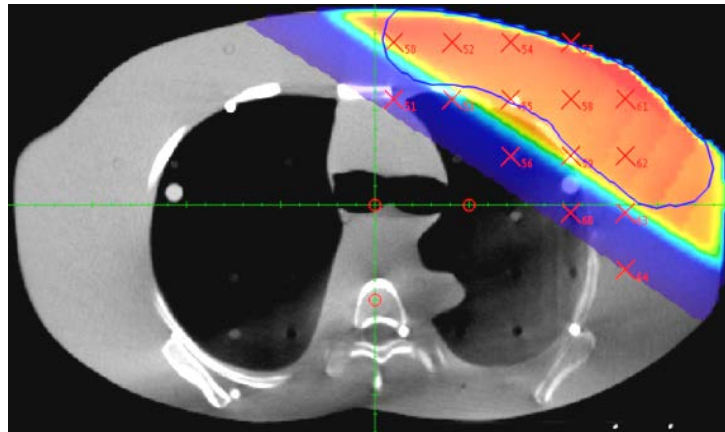
Figures 8-11 show the distribution of TLDs in the phantom. Markings in red indicate TLDs inserted in the planning system. Points circled in white indicate the proper placement of TLDs, experimentally. In these figures, the area with higher reliability is the red one, followed by the yellow zone, and finally, by the blue zone, with the lowest reliability, based on the isodose curves assessed by the planning system.

Tables 1-4 show the comparison of absorbed and planned doses for each slice, where a relative standard deviation of up to 6% is observed.

Whereas the planning was done by placing the point of interest for the treatment of male breast cancer near TLD L01, located at position 10 of slice 16, the percentage error shown relative to the plan was of 0.3%. That is, the planning coincides with the measurements expressed by TLDs, in the dose distribution for the treatment performed.

In Table 1, there is a difference of approximately 25 cGy for TLD plan number 63, however, the dose planned for this TLD was of 42.4 cGy and the calibration curve of TLDs is not reliable for measurements inferior to 50 cGy. We can also see a difference of approximately −21 cGy for the TLD plan number 55, however, it was located in a transition area and this location may show results different than planned, since reliability was changed and a 1 mm difference in location, from actual to planned, may generate significantly discrepant results. TLD plan number 52, on the other hand, shows a difference of approximately −13 cGy between the actual dose and the planned dose, but if we evaluate it proportionally, when compared to the average dose, this difference does not exceed 6.3%.

As shown in Table 2, slice 16 is the one with smaller relative standard deviations and smaller differences between planned and actual doses, when compared to other slices, precisely because planning focused on this slice.

Figure 8. Distribution of TLDs in the planning system in red and experimental TLDs circled in slice 15.
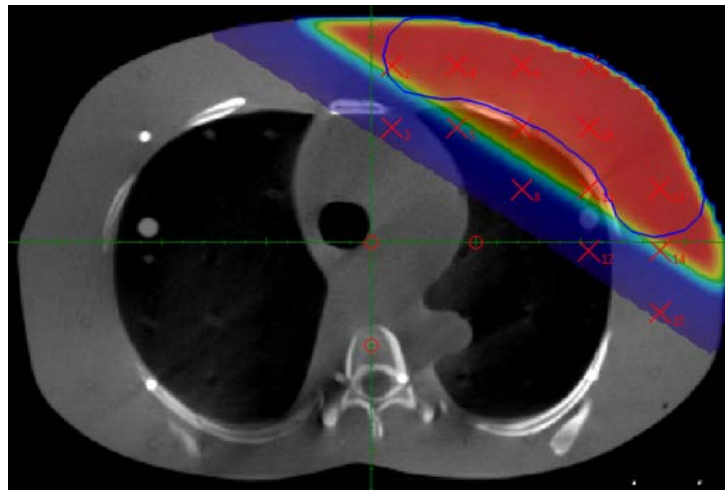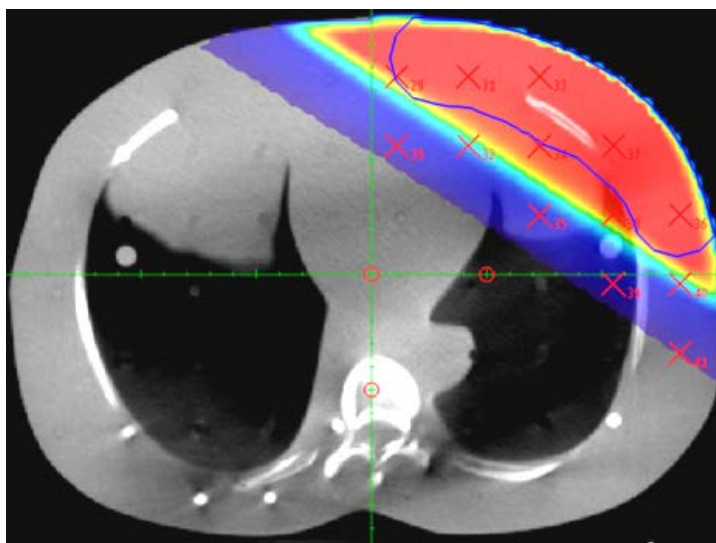

Figure 9. Distribution of TLDs in the planning system in red and experimental TLDs circled in slice 16.
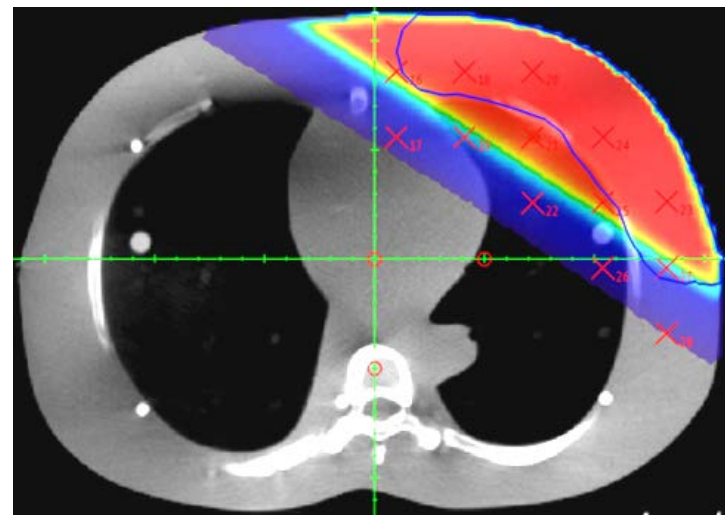
Figure 10. Distribution of TLDs in the planning system in red and experimental TLDs circled in slice 17.

Figure 11. Distribution of TLDs in the planning system in red and experimental TLDs circled in slice 18.

Table 1. Comparison between doses absorbed by TLDs and doses planned in slice 15.

			Comparison between Corrected Doses (*cGy*)								
TLD	TLD Plan	Planned Dose	Measurement			Average	Standard Deviation	Relative Standard Deviation	Ua	Zone*	Real/Planned Dose
			1	2	3						
e02	52	187.78	214.23	193.15	193.65	200.34	12.03	6%	6.94	R	−12.56
e05	55	176.35	194.88	197.26	199.41	197.19	2.26	1%	1.31	Y	−20.84
b01	58	181.31	207.40	194.13	197.78	199.77	6.85	4%	3.96	R	−18.46
n03	61	189.25	200.78	193.54	192.97	195.76	4.35	2%	2.51	R	−6.51
d14	63	42.4	16.59	18.15	17.96	17.57	0.85	2%	0.49	B	24.83

*R—red; Y—yellow; B—blue.

Table 2. Comparison between doses absorbed by TLDs and doses planned in slice 16.

			Comparison between Corrected Doses (*cGy*)								
TLD	TLD Plan	Planned Dose	Measurement			Average	Standard Deviation	Relative Standard Deviation	Ua	Zone*	Real/Planned Dose
			1	2	3						
c04	4	197.45	203.46	204.70	198.62	202.26	3.21	2%	1.86	R	−4.81
d20	6	202.47	218.05	208.29	198.91	208.41	9.57	5%	5.53	R	−5.94
h16	8	19.05	16.67	16.51	15.70	16.29	0.52	3%	0.30	B	2.76
l01	10	199.45	204.82	198.26	193.67	198.92	5.60	3%	3.24	R	0.53
o02	12	13.75	12.86	12.73	12.77	12.78	0.06	0%	0.04	B	0.97
h09	13	205.29	206.97	206.22	213.25	208.81	3.86	2%	2.23	R	−3.52
n04	15	4.45	9.24	8.94	8.76	8.98	0.24	5%	0.14	B	−4.53

*R—red; B—blue.

Table 3. Comparison between doses absorbed by TLDs and doses planned in slice 17.

			Comparison between Corrected Doses (*cGy*)								
TLD	TLD Plan	Planned Dose	Measurement			Average	Standard Deviation	Relative Standard Deviation	Ua	Zone[*]	Real/Planned Dose
			1	2	3						
h07	17	14.01	12.29	12.28	11.66	12.08	0.36	3%	0.21	B	1.93
e03	18	199.73	200.89	207.14	207.03	205.02	3.58	2%	2.06	R	−5.29
i11	20	207.1	212.90	228.30	223.41	221.54	7.87	4%	4.54	R	−14.44
b15	21	190.35	202.00	204.58	200.47	202.35	2.07	1%	1.20	R	−12.00
n20	24	203.82	197.92	222.80	205.16	208.63	12.79	6%	7.39	R	−4.81
e06	27	48.2	23.30	22.65	24.04	23.33	0.69	1%	0.40	B	24.87

[*]B—blue; R—red.

Table 4. Comparison between doses absorbed by TLDs and doses planned in slice 18.

			Comparison between Corrected Doses (*cGy*)								
TLD	TLD Plan	Planned Dose	Measurement			Average	Standard Deviation	Relative Standard Deviation	Ua	Zone[*]	Real/Planned Dose
			1	2	3						
o20	32	53.29	25.13	27.67	27.61	26.80	1.45	3%	0.84	B	26.49
o14	35	20.03	15.26	14.41	13.74	14.47	0.76	4%	0.44	B	5.56
h08	37	204.16	216.37	228.56	224.50	223.14	6.21	3%	3.58	R	−18.98
n10	39	14.24	11.59	11.39	11.71	11.56	0.16	1%	0.09	B	2.68
o20	32	53.29	25.13	27.67	27.61	26.80	1.45	3%	0.84	B	26.49

*B—blue; R—red.

Table 3 shows a difference of approximately 25 cGy for TLD plan number 27, however, this TLD has a planned dose of 48.2 cGy and the calibration curve of TLDs is also not reliable for measurements inferior to 50 cGy. We also notice a difference of approximately −15 cGy for TLD plan number 20 and of −12 cGy for TLD plan number 21, between the actual and the planned doses, but, proportionately, in relation to average doses, these differences do not exceed −6.5%.

In **Table 4**, there is a difference between the planned and the actual dose of up to 26 cGy, which may be associated with the location of the TLDs, which were in the blue zone, and because of the error existing in the calibration curve, for doses inferior to 50 cGy. We can also notice a difference of approximately −19 cGy for TLD plan number 37, between the actual and the planned dose; however, if we evaluate in terms of average dose, this difference means approximately −8.5% of the measured average dose.

4. Conclusion

We may conclude that the volume of the male breast directly impacts the results diverging from planning. Thus, it is necessary to study and program a specific plan for the treatment of male breast cancer. The adoption of the same protocols used for the treatment of female breast cancer is not recommended.

Acknowledgements

References

[1] Paiva, S.M.M. (2006) Avaliação da qualidade de vida de pacientes oncológicos em tratamento quimioterápico adjuvante. Dissertação, Ribeirão Preto, 111 p.

[2] Hill, T.D., Khamis, H. J., Tyczynski, J.E. and Berkel, H.J. (2005) Comparison of Male and Female Breast Cancer Incidence Trends, Tumor Characteristics, and Survival. *Annals of Epidemiology*, **15**, 773-780. http://dx.doi.org/10.1016/j.annepidem.2005.01.001

[3] Giordano, S.H. (2005) A Review of the Diagnosis and Management of Male Breast Cancer. *Oncologist*, **7**, 471-479. http://dx.doi.org/10.1634/theoncologist.10-7-471

[4] Carmalt, H.L., Mann, L.J., Kennedy, C.W., Fletcher, J.M. and Gillet, D.J. (1998) Carcinoma of the Male Breast: A Review and Recommendations for Management. *ANZ Journal of Surgery*, **68**, 712-715. http://dx.doi.org/10.1111/j.1445-2197.1998.tb04657.x

[5] Leme, L.H.S. and Souza, G.A. (2006) Câncer de mama em homens: Aspectos epidemiológicos, clínicos e terapêuticos. *Revista de Ciências Médicas*, **15**, 391-398.

[6] Izewska, J. and Rajan, G. (2005) Chapter 3: Radiation Dosimeters. In: Podgorsak, E.B., Ed., *Radiation Oncology Physics*: *A Handbook for Teachers and Students*, International Atomic Energy Agency-IAEA, Vienna.

[7] Da Rosa, L.A.R. (2001) Dosimetria Termoluminescente Aplicada à Física Médica, Instituto de Radioproteção e Dosimetria-CNEN, Rio de Janeiro.

[8] ICRU (1989) International Commission on Radiation Units and Measurements. Tissue substitutes in radiation dosimetry and measurement, Report 44, Bethesda.

[9] Guimarães, N.A. and Crispim, V.R. (2013) Dosimetric Evaluation in Teletherapy to Treatment of Male Breast. *International Nuclear Atlantics Conference*, Pernambuco.

Scientific Research Publishing (SCIRP) is one of the largest Open Access journal publishers. It is currently publishing more than 200 open access, online, peer-reviewed journals covering a wide range of academic disciplines. SCIRP serves the worldwide academic communities and contributes to the progress and application of science with its publication.

Other selected journals from SCIRP are listed as below. Submit your manuscript to us via either submit@scirp.org or Online Submission Portal.